14th International Conference on CFD in Oil & Gas, Metallurgical and Process Industries
SINTEF, Trondheim, Norway
June 9–11, 2020

TO QUANTIFY MIXING QUALITY IN A SINGLE SCREW EXTRUDER SIMULATION

TJ Mateboer*, C Hummel, DJ van Dijk, J Buist

Windesheim University of Applied Sciences, Professorship for Polymer Engineering, P.O. Box 10090, 8000 GB Zwolle, The Netherlands

* E-mail: t.j.mateboer@windesheim.nl

ABSTRACT

Polymer mixing with a single screw extruder is a common process in industry. Mixing quality depends on (amongst others) the screw geometry. The main objective of this study was to quantify distributive mixing behavior of a single screw extruder with computational fluid dynamics (CFD) simulations.
Tracer particles and Shannon entropy calculations were used to determine the distributive mixing quality as function of direction, position in the extruder and scale of observation.
The distributive mixing quality was determined for 3 different simulations of a mixing section (the spiral Maddock) of a single screw extruder. The mixing quality depends on both the angular and radial inflow position of the tracer particles. The different simulations show different mixing quality in angular direction. The different simulations did not show much difference in mixing quality in the radial direction.

Keywords: CFD, Polymer mixing, distributive mixing, single screw extruder, Non-Newtonian fluid dynamics, Shannon entropy, Numerical simulation, spiral Maddock

NOMENCLATURE

Greek Symbols

$\dot{\gamma}$	Shear rate, [s^{-1}].
η	Viscosity, [Pa·s].
η_0	Viscosity at zero shear rate, [Pa·s].
η_∞	Viscosity at infinite shear rate, [Pa·s].
λ	Relaxation time, [s].
τ	Shear stress, [Pa].

Latin Symbols

c_i	Number of particles in bin *i*, [-].
i	Bin number, [-].
M	Number of bins, [-].
m	Flow consistency index, [Pa·s^{-n}].
N	Total number of tracer particles, [-].
n	Power law index, [-].
p_i	Probability of a particle to flow through bin *i*.
S_{rel}	Relative Shannon entropy, [-].

INTRODUCTION

Polymer mixing with a single screw extruder is a common process in industry. Mixing quality is often divided into dispersive and distributive mixing. With distributive mixing the additive units or the discontinuous phase are/is homogeneously distributed throughout the polymer. Mixing quality depends on (amongst others) the screw geometry. Specialized mixing sections in a screw geometry are necessary for a high mixing quality with a single screw extruder. The spiral Maddock is such a mixing section.

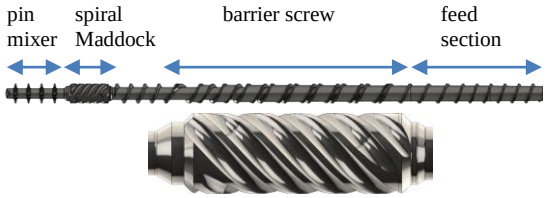

Figure 1: Upper: Extruder screw with four section. Fluid flow is from right to left. Lower: spiral Maddock section.

A more efficient mixing screw geometry may be determined with computational fluid dynamics (CFD) simulations. Several studies have modeled polymer mixing with computational fluid dynamics (CFD) (1-13). Distributive mixing behavior in simulations is often quantified with a residence time distribution (RTD) of tracer particles (1, 5, 14-18). And with the Shannon entropy (6, 8, 15, 16, 19, 20). These methods often result in limited information of:

- Mixing quality in different direction (angular and radial directions) separately.
- Mixing quality at different positions in the extruder.
- Mixing quality at both a large and small scale of observation

In this study the Shannon entropy was used to calculate distributive mixing quality as function of position in the extruder, as function of direction and as function of scale.
The mixing quality of several extrusion simulations were calculated to determine how well a distinction in

mixing quality can be made with the Shannon entropy. Only mixing quality was calculated, the study does not show an optimized screw geometry. Furthermore only the spiral Maddock screw section was included in the simulations.

SIMULATION SETUP

Three extrusion simulations with the spiral Maddock were performed. The method for determining mixing quality is shown in this section. The simulations were performed with the immersed solid method (ISM) in CFX (Ansys 19.2). All the simulations are steady state and isothermal.

Spiral Maddock geometry

The spiral Maddock is a mixing section of a single screw extruder with a 75 mm diameter, see Figure 1. The spiral Maddock is designed for dispersive mixing. In this study only the distributive mixing quality is calculated, not the dispersive mixing quality.
The spiral Maddock consist of several flights, inflow and outflow channels. The spiral Maddock is discrete rotational symmetrical along the rotational axis.

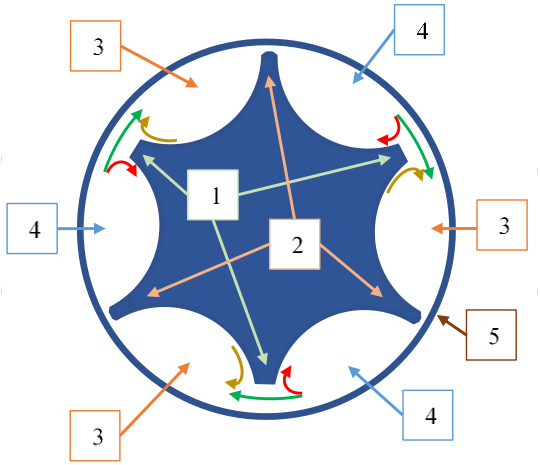

Figure 2: Schematic cross section of a spiral Maddock. 1: barrier flights. 2: main flights. 3: outflow channels. 4: inflow channels. 5: barrel wall.

The spiral Maddock is designed so that the fluid passes through a gap between the barrier flight and the barrel. The barrier flight height was varied so that the gap between the barrier flight and the barrel and the was 1.74 mm or 0.74 mm.
The gap between the main flight and the barrel wall is very narrow in order to prevent fluid to flow through this gap. This size of this gap makes meshing difficult. Therefore the main flight was extended beyond the barrel wall. With this setup the gap between the main flight and the barrel wall does not exist in the simulations.

Boundary conditions

A no slip condition was set on both the barrel and screw walls. The screw rotates relative to the barrel wall. A mass flow rate condition was set to 0.015 kg/s. A 0 Pa conditions was set at the outflow opening.

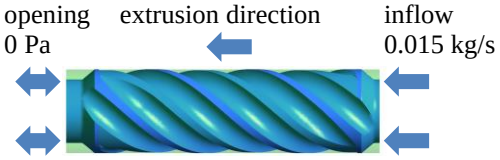

Figure 3: Side view of the spiral Maddock. The screw (ISM) is in blue, the fluid domain is in green.

Simulations were performed with a screw rotational velocity of 1.5 rad/s and 4.6 rad/s.

Material parameters

The material parameters were derived from a HDPE (Marlex TRB-432, Chevron Phillips Chemical Company). The viscosity as function of shear rate was determined with a capillary rheometer at 200 °C. Measurements were performed in a shear rate range from $\dot{\gamma} = 4\,\mathrm{s}^{-1}$ up to $\dot{\gamma} = 500\,\mathrm{s}^{-1}$. A power law was fitted onto the rheological measurements with n = 0.35 and m = $3.3 \cdot 10^4$ Pa·s^{-n}.
Power law

$$\tau = m\dot{\gamma}^n \qquad (1)$$

For numerical stability a Bird-Carreau model was used in the simulations:
Bird-Carreau model

$$\eta = \eta_\infty + (\eta_0 - \eta_\infty)\left(1 + (\lambda\dot{\gamma})^2\right)^{\frac{n-1}{2}} \qquad (2)$$

The viscosity at infinite shear rate (η_∞) is 1 Pa·s, the viscosity at zero shear rate (η_0) is 3 MPa·s. The relaxation time (λ) is 1000 s. The Bird-Carreau and the power law show are almost identical in the shear rate range of $\lambda^{-1} > \dot{\gamma} > \left(\frac{\eta_\infty}{m}\right)^{\frac{1}{n-1}}$. λ and η_∞ are chosen so that the power law and the Bird-Carreau show similar behavior at $10^{-3} > \dot{\gamma} > 10^7$. This range seems reasonable since lower and higher shear rates were not expected to have a significant influence on the simulation. Furthermore no rheological measurements were available at those low and high shear rates.

Mesh

A fluid domain and an immersed solid were created.

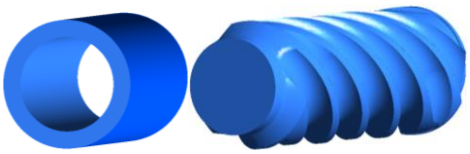

Figure 4: Left: fluid domain. Right: immersed solid domain (spiral Maddock).

The two domains were meshed separately. The fluid domain mesh consists of a part with cubical cells near the barrel wall.

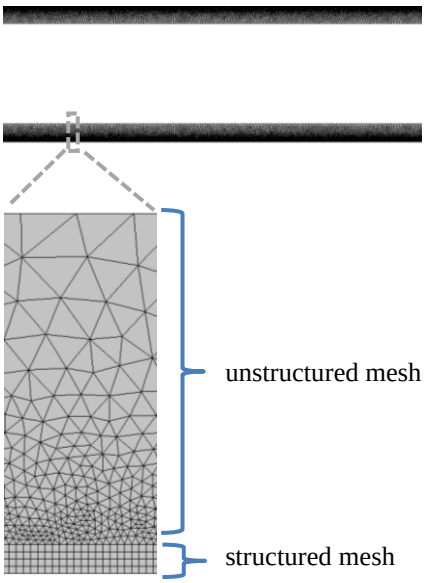

Figure 5: Cross section of a fluid domain mesh.

The height of this structured part is similar in size to the gap between the barrier flight and the barrel. This ensures a minimum number of cells between the barrier flight and the barrel wall. A large aspect ratio in these cells resulted in numerical instabilities, therefore the structured cells are cubical.
The rest of the fluid domain consists of an unstructured mesh. A simulation with a proper mesh density does not change when the mesh cell density is increased. Therefore a mesh study was conducted. The cell size of the cubical cells were incrementally reduced from an average cell size of 0.15 mm down to 0.05 mm. The unstructured cell was reduced in size accordingly. The total number of cells increased from 58 M up to 479 M. Simulations with the different meshes were compared by comparing the pressure at the inflow of the spiral Maddock.
The immersed solid domain / screw mesh size does not have a great impact on the computational costs. Therefore a single fine mesh was made of the screw. This unstructured mesh was used in each simulation.

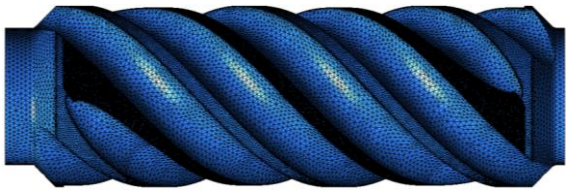

Figure 6: Side view of the immersed solid domain mesh / screw mesh.

It is preferred to have a well-defined gap between the barrel and the barrier flight. Therefore the barrier flight back has a very fine mesh.

Tracer particles

The flow paths of the fluid determines distributive mixing. The flow paths can be determined with tracer particles. The tracer particles were introduced after the simulation. The path of each particle is determined by calculating the next particle position with the velocity and trajectory of the fluid at the current particle position.

Mixing is expected to be discrete rotational symmetrical since the spiral Maddock is discrete rotational symmetrical. Therefore 10^5 particles are introduced equally spaced into 1/3 of the inflow boundary equally divided.

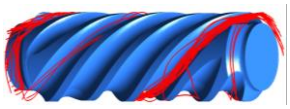

Figure 7: Example of small number of tracer particles introduced in the spiral Maddock simulation.

Variation in the simulation setup

3 different simulation were executed. The configuration are shown in Table 1.

Table 1: Modelling conditions.

simulation name	screw rotational velocity	Gap between the barrier flight and the barrel
standard	1.5 rad/s	0.74 mm
high screw velocity	4.6 rad/s	0.74 mm
lowered barrier flight	1.5 rad/s	1.74 mm

The standard setup was used for the mesh study. Mixing quality was calculated for all three the setups. The purpose of the different setups is to determine how well a distinction in mixing quality can be made with the Shannon entropy. The setups were not chosen to determine a optimal extrusion setup or screw geometry.

SHANNON ENTROPY

Shannon entropy is a single measure to determine a distribution across a number of bins (M). Relative Shannon entropy (S_{rel}) is calculated with the probability (p_i) that a tracer particle flows through a bin.
Relative Shannon entropy

$$S_{rel} = \frac{-\sum_{i=1}^{M} p_i \ln p_i}{\ln M} \qquad (3)$$

In this document Shannon entropy is used as short for 'relative Shannon entropy'. p_i is equal to the number of tracers (c_i) in bin i divided by the total number of tracer particles (N).
A low relative Shannon entropy corresponds to a low mixing quality. Maximum Shannon entropy and maximum mixing quality is reached when $S_{rel} = 1$. The Shannon entropy is in the range $0 < S_{rel} \leq 1$, which makes it possible to estimating mixing quality. The Shannon entropy was calculated at the outflow side of the spiral Maddock. Therefore the outflow was divided into several bins.

Bin division schemes

The orientation of the bin division scheme determines the direction of mixing quality that can be calculated with the Shannon entropy. Mixing quality in an angular direction can be calculated with an angular bin division scheme. Mixing quality in a radial direction can be calculated with a radial bin division scheme.

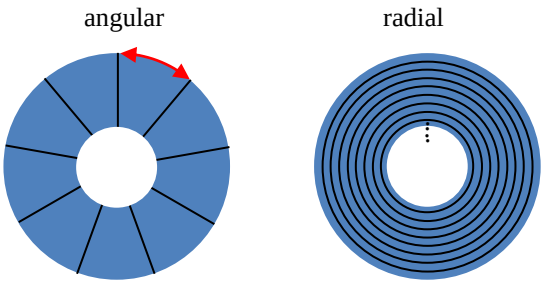

Figure 8: Schematic of bin distribution schemes. Left: angular divisions. Right: radial division.

The above schematic shows two bin division with 8 bins. The typical size of the angular bins is the circumference divided by the number of bins (*M*), see the red arrow in the above figure. The typical size of the radial bins is the distance between the screw and the barrel divided by the number of bins (*M*).
Mixing quality at a macroscopic level can be determined with a small number of bins. Mixing quality on a microscopic level can be determined with a large number of bins. From 3 up to 96 bins were used to calculate a Shannon entropy.

Tracer particle inflow sections

The tracer particles were introduced equally divided across 1/3 of the inflow. Therefore the mixing quality was already very high when all the particles would be included in the calculations. Not all particles are included in calculating a Shannon entropy, the inflow was divided into section with the same size and shape as the outflow bins. Shannon entropy was only calculated with the particles from a single section at the inflow. The Shannon entropy can be calculated for each inflow section independently.

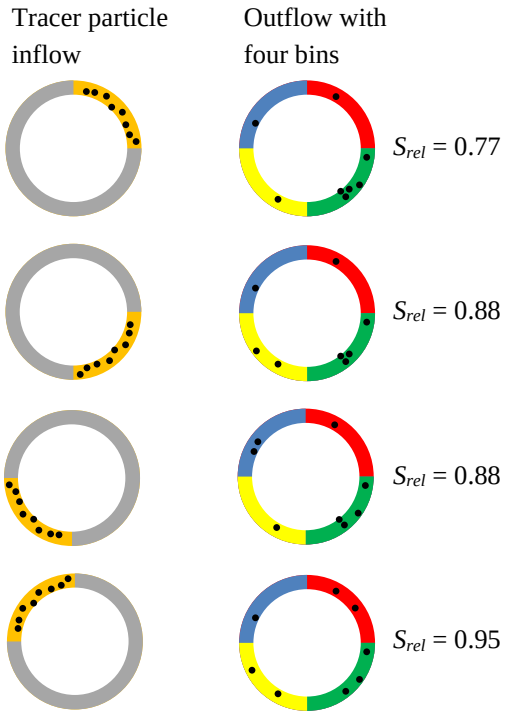

Figure 9: A hypothetical example of four Shannon entropy calculations with an angular bin division scheme. Each Shannon entropy is calculated with another section for introducing the tracer particles.

Figure 9 shows an example for an angular bin division scheme. The example shows 4 bins. The inflow sections have the same size as the bins, therefore the inflow (in the example) is divided into 4 section. A different Shannon entropy can be calculated for each inflow section.
Multiple inflow section can also be used with a radial bin division scheme. But then the inflow is divided up in a radial direction. With this method the Shannon entropy as function of position (angular and radial) can be calculated.
Dividing the particles across the inflow section reduces the number of particles per Shannon entropy calculation. It seems reasonable that a lower number of particles per bin results in an increase in uncertainty in the Shannon entropy. Therefore the average number of particles per bin is at least 30.
All the Shannon entropy calculation were performed with GNU Octave.

RESULTS

Mesh study

Simulations with the different meshes were compared with the pressure at the inflow of the spiral Maddock.

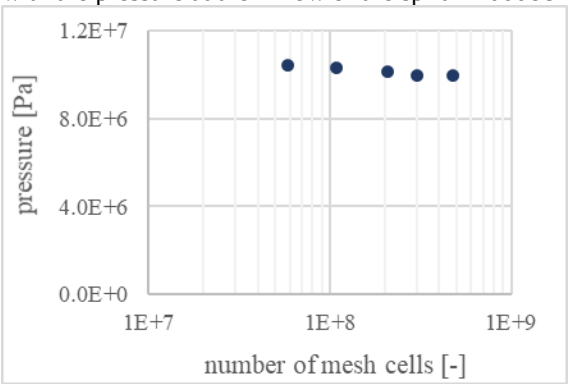

Figure 10: Pressure at the inflow of the spiral Maddock as function of mesh size.

The pressure does not reduce much with increase of mesh size. Therefore the most coarse mesh (58 M cells) was used to determine mixing quality.

Particle distribution

10^5 tracer particles were introduced at the inflow. The tracer particle positions at the outflow are shown in Figure 11.

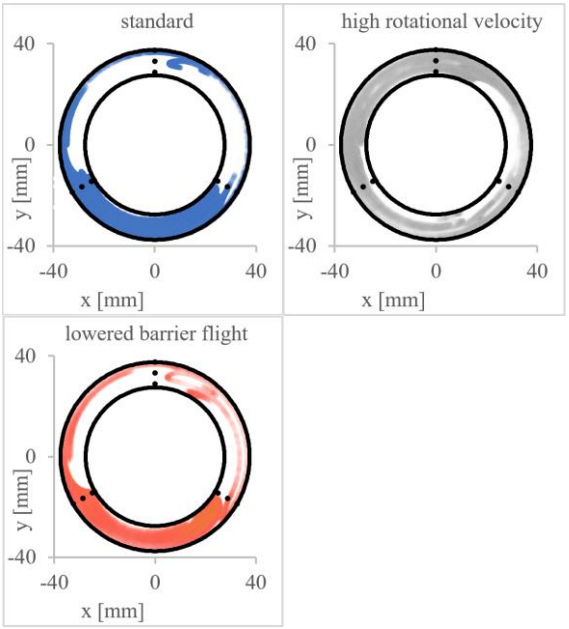

Figure 11: Tracer particles positions at the outflow of the spiral Maddock. The particles are colored dots angular bins are marked with dotted lines.

The figure allows for a visual estimation of the mixing quality. The simulation with a high rotational screw velocity seems to have a higher mixing quality compared to the other simulation. The standard and lowered barrier flight show a very similar particle distribution.

Angular distributive mixing quality

The inflow of the spiral Maddock was divided up into section in an angular direction. Tracer particles were introduced in each section and the Shannon entropy was calculated. Figure 12 shows the Shannon entropy as function of inflow section with an angular bin division scheme.

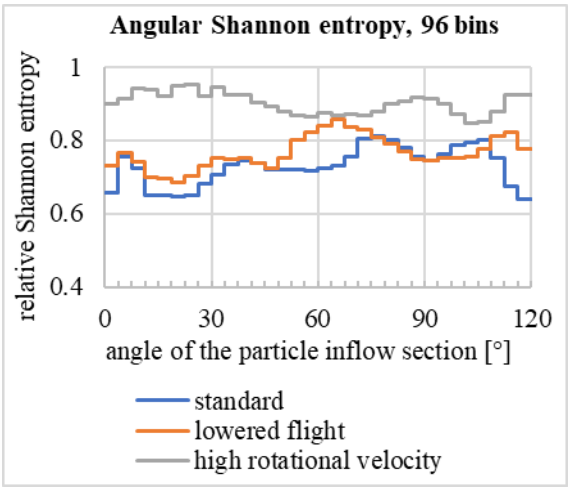

Figure 12: Shannon entropy as function of inflow section with an angular bin division scheme and a typical bin size of 2.5 mm.

A high Shannon entropy corresponds to a high distributive mixing quality while a low Shannon entropy corresponds to a low distributive mixing quality. The angular mixing quality depends on the tracer particle inflow section. For example the lowered flight simulation: the mixing quality is better with inflow section at 60.75°-67.50° (S_{rel} = 0.86) while the mixing quality is less (S_{rel} = 0.73) with the inflow section at 0°-3.75°. The high rotational velocity shows a higher mixing quality. The above figure only shows the results with a typical bin width of 2.5 mm. A minimum or an average mixing quality of all inflow section can be used to show mixing quality at other scales of observation.

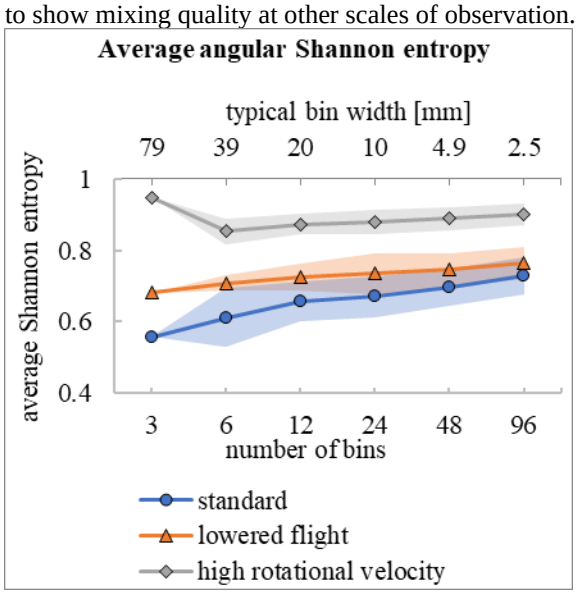

Figure 13: Average angular Shannon entropy as function of number of bins (bottom axis) and typical bin width (top axis). The colored bands show the standard deviation. Note: the horizontal axis is on a logarithmic scale.

The high rotational velocity simulation shows a higher average Shannon entropy compared to the other simulations. And therefore the high rotational velocity shows a higher distributive mixing quality. The lowered flight simulation show a bit higher average angular mixing quality compared to the standard simulation at each typical bin width. Although there is an overlap when the standard deviation is taken into account. The mixing quality of the simulations can also be compared with the minimum Shannon entropy of a simulation at a specific typical bin width.

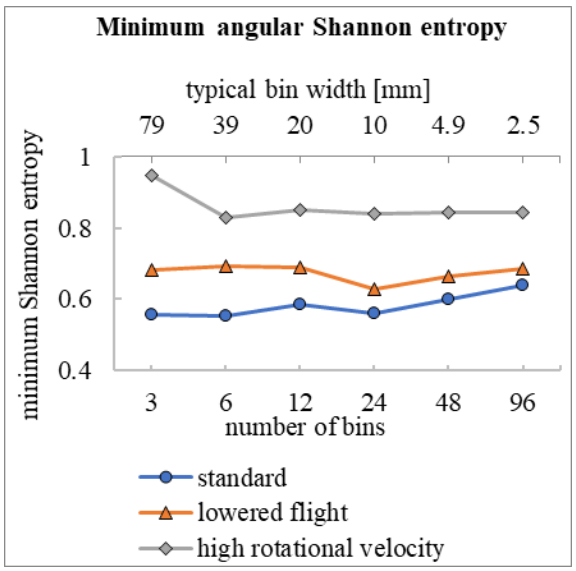

Figure 14: Minimum angular Shannon entropy as function of number of bins (bottom axis) and typical bin width (top axis). The colored bands show the standard deviation. Note: the horizontal axis is on a logarithmic scale.

Comparing the minimum Shannon entropy is useful for a design study when a minimum mixing quality is required. The lowest angular mixing quality of the lowered flight simulation is better than the lowest mixing quality of the standard simulation at all typical bin widths.

Radial distributive mixing quality

Shannon entropy was calculated with a radial bin division scheme. The inflow was divided up into radial section. Figure 15 shows the Shannon entropy as function of radial inflow section.

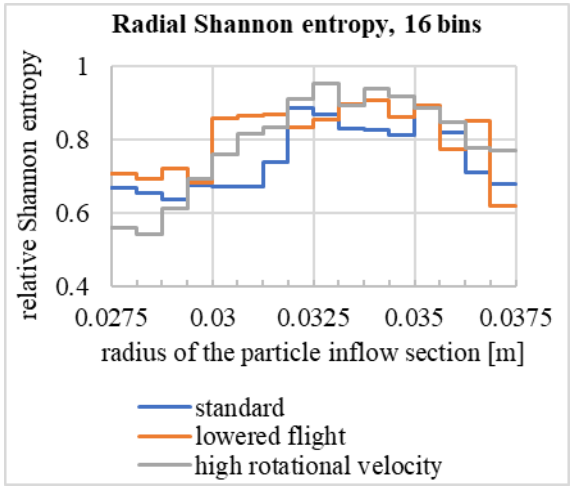

Figure 15: Shannon entropy as function of inflow section with a radial bin division scheme and a typical bin size of 0.6 mm.

The distributive mixing quality in the radial direction does depend on the radial position of the particle inflow section. The mixing quality depends more on the inflow position than on the simulation setups included in this study. Therefore it is not meaningful to make a comparison of average or minimum Shannon entropy as was done with the angular bin distribution.

CONCLUSION AND RECOMMENDATIONS

Tracer particles and Shannon entropy calculations were used to determine the distributive mixing quality as function of:

- radial and angular direction
- scale of observation
- radial and angular inflow position of the tracer particles

The distributive mixing quality was determined for 3 different simulations of a spiral Maddock. The mixing quality depends on both the angular and radial inflow position of the tracer particles. The different simulations show different mixing quality in angular direction. The simulations did not show a difference in mixing quality in a radial direction.
The difference, between the simulation, in mixing quality was not determined for the radial direction.

Recommendation / future work

In this study only a single mixing section of an extruder was included (the spiral Maddock). Furthermore these simulations were not verified with experiments. Future work will focus on verifying the simulations with experiments. Specifically the distributive mixing quality of the simulations. Furthermore future work will also focus on including the whole screw and the extruder die.

ACKNOWLEDGEMENTS

This study was financially supported by Tech For Future (TFF) and Wavin T&I. The Windesheim University Professorship for Polymer Engineering conducted this study with Wavin T&I. Wavin T&I provided expert advice, essential equipment, materials and experimental data.

REFERENCES

1. Zong Y, Tang H, Zhao L. 3-D numerical simulations for polycondensation of poly(p-phenylene terephthalamide) in twin screw extruder. Polymer Engineering and Science. 2017;57(11):1252-61.
2. Tang H, Zong Y, Zhao L. Numerical simulation of micromixing effect on the reactive flow in a co-rotating twin screw extruder. Chinese Journal of Chemical Engineering. 2016;24(9):1135-46.
3. Zhang XM, Xu ZB, Feng LF, Song XB, Hu GH. Assessing local residence time distributions in screw extruders through a new in-line measurement instrument. Polymer Engineering & Science. 2006;46(4):510-9.
4. Zhang XM, Feng LF, Hoppe S, Hu GH. Local residence time, residence revolution, and residence volume distributions in twin-screw extruders. Polymer Engineering & Science. 2008;48(1):19-28.
5. Zhang XM, Feng LF, Chen WX, Hu GH. Numerical simulation and experimental validation of mixing performance of kneading discs in a twin screw extruder. Polymer Engineering & Science. 2009;49(9):1772-83.
6. Manas-Zloczower I, Kaufman M, Alemaskin K, Camesasca M. Color Mixing in Extrusion: Simulations and Experimental Validation.
7. Alemaskin K, Manas-Zloczower I, Kaufman M. Color mixing in the metering zone of a single screw extruder: numerical simulations and experimental validation. Polymer Engineering & Science. 2005;45(7):1011-20.
8. Alemaskin K, Manas-Zloczower I, Kaufman M. Entropic analysis of color homogeneity. Polymer Engineering & Science. 2005;45(7):1031-8.

9. Alemaskin K. Entropic Measures of Mixing in Application to Polymer Processing: Case Western Reserve University; 2004.
10. Alemaskin K, Camesasca M, Manas-Zloczower I, Kaufman M, editors. Entropic measures of mixing tailored for various applications. AIP Conference Proceedings; 2004: AIP.
11. Alemaskin K, Camesasca M, Manas-Zloczower I, Kaufman M, Kim E, Spalding MA, et al., editors. Entropic mixing characterization in a single screw extruder. SPE ANTEC; 2004.
12. Alemaskin K, Manas–Zloczowe I, Kaufman M. Index for simultaneous dispersive and distributive mixing characterization in processing equipment. International Polymer Processing. 2004;19(4):327-34.
13. Alemaskin K, Manas-Zloczower I, Kaufman M, editors. Simultaneous characterization of dispersive and distributive mixing in a single screw extruder. Proceedings of the Int Conf ANTEC; 2003.
14. Wang W, Zloczower I, editors. Dispersive and distributive mixing characterization in extrusion equipment. Antec 2001 Conference Proceedings; 2001.
15. Tadmor Z, Gogos CG. Principles of Polymer Processing: Wiley; 2006.
16. Xu B, Yu H, Kuang T, Turng LS. Evaluation of Mixing Performance in Baffled Screw Channel Using Lagrangian Particle Calculations. Advances in Polymer Technology. 2017;36(1):86-97.
17. Yamada S, Fukutani K, Yamaguchi K, Funahashi H, Ebata K, Uematsu H, et al. Dispersive mixing performance evaluation of special rotor segments in an intermeshing co-rotating twin-screw extruder by using weighted probability distributions. International Polymer Processing. 2015;30(4):451-9.
18. Chen J, Cao Y, editors. Simulation of 3D flow field of RPVC in twin-screw extrusion under wall slip conditions. Proceedings of 2012 9th International Bhurban Conference on Applied Sciences and Technology, IBCAST 2012; 2012.
19. Wang W, Manas-Zloczower I, Kaufman M. Entropic characterization of distributive mixing in polymer processing equipment. AIChE Journal. 2003;49(7):1637-44.
20. Manas-Zloczower I, Agassant JF. Mixing and Compounding of Polymers: Theory and Practice: Hanser; 2009.